Chapter 2

Theoretical Considerations

2.1 Introduction:

The present thesis deals with the study of Hyperfine interactions in some dilute alloys and high T_c superconducting compounds (HTSC). The Mossbauer spectroscopic technique is used to study out the various interactions of the probe nucleus and the surrounding. A brief theory of Mossbauer effect is given. The Electric Field Gradient in metals is due to the asymmetric spatial charge distribution. Hence it provides microscopic information about charge distribution in metals. Also magnetic hyperfine interactions arise from the interaction of nuclear magnetic dipole moment and the magnetic field due to atom's own electrons. The theoretical aspects of these different effects are briefly discussed in this chapter.

2.2 Mössbauer Effect:

The Mössbauer effect is based on the phenomenon of emission and resonance absorption of γ-rays without any loss in energy due to recoil of the nucleus. The nuclei of a fraction of atoms, which are bound to the crystal lattice, can absorb and also emit γ- ray without the loss of energy due to the recoil and Doppler broadening. This phenomenon is known as Mössbauer effect and was discovered by R.L Mossbauer in 1958 (1). This technique has a high resolving power than most of the other spectroscopic techniques. Hence Mössbauer technique has variety of applications in Solid State Physics, Nuclear Physics, Relativity, Geology, Chemistry, Biology, Medicine, Archeology etc. The high resolution makes this technique a very important tool to find out the changes in the energy difference of the order of 10^{-8} eV, found in hyperfine splitting of nuclear levels.

A brief discussion of the phenomenon of the Mössbauer effect and different parameters that can be obtained from this technique are given below :

2.3 Principles of Mössbauer Effect:

The Mössbauer effect is based on the principle of recoilless emission and resonance absorption of γ-rays. A photon is emitted if a nucleus is making a transition from one state to another of lower energy. The reverse process can also take place when the system has right energy to make a transition to a higher state. This process is known as resonance absorption. But whenever the nucleus of a free atom at rest emits γ-ray photon it recoils. The kinetic energy associated with this recoil is given by

$$R = \frac{E_0^2}{2mc^2},$$

Where E_0 is the energy of the nuclear transition,

m is the mass of the atom,

c is the velocity of light.

The emitted γ-ray will thus have energy

$$E_\gamma = E_o - R.$$

Similarly for absorption process in nucleus, for resonant absorption the photon should have energy

$$E\gamma' = E_o + R$$

Due to Doppler broadening the width of the emission and absorption lines becomes

$$\Delta = 2(E_R K_B T)^{1/2}$$

Where K_B is the Boltzman's constant,

T is the absolute temperature of the source and the absorber.

For resonance fluorescence to take place the Doppler broadening should be larger than $2E_R$. In atomic systems this condition is satisfied in a natural way, but for nuclear processes even with Doppler broadening it is difficult to get resonance. In 1958, Mössbauer demonstrated that resonance fluorescence of γ-rays is possible if both emitting and absorbing nuclei are bound with in the solid. In this case the solid as a whole or the lattice takes the recoil momentum of the emitting nuclei.

If the emitting or the absorbing nuclei embedded in the lattice, the recoil momentum is transferred to the lattice or whole crystal. As vibrational energy levels of the lattice are quantised, the recoil energy corresponding to the allowed vibrational energy can only be transferred to the lattice. This energy transfer can cause excitation with in the solid by creation or destruction of phonons. Hence a probability distribution for energy transferred to the lattice exists. The emission or absorption of the γ-ray, which results in zero-phonon in solids, shows the Mössbauer Effect.

Also the average recoil energy must be smaller than the phonon transitions. For a solid:

$K_B\theta_D$ is used as typical phonon energy

Where θ_D is the Debye temperature of the Solids.

If $E_R < K_B \theta_D$ a large fraction of the γ-rays will produce zero phonon transition. With rise in temperature more and more phonons will be excited resulting in less and less zero phonon processes.

The probability distribution of zero phonon emission and absorption process can be calculated by assuming a gaussian distribution for atom with mean square vibrational amplitude of the emitting atom $<X^2>$ in the direction of recoil fraction (f).

Thus

$$f = \exp(-K^2<X^2>)$$

In Debye model of the lattice vibration, recoil free fraction is given by

$$f = \exp\left\{\frac{-6E_R}{K_B\theta_D}\left[\frac{1}{4}+\left(\frac{T}{\theta_D}\right)^2\int_0^{\frac{\theta_D}{T}}\frac{xdx}{e^x-1}\right]\right\}$$

This equation can be written as

$$f = \exp(-2W)$$

Where W is called the Debye Waller factor.

At very low temperature, $T \ll \theta_D$, the f fraction reduces to

$$f = \exp-\left[\frac{E_R}{K_B\theta_D}\left(\frac{3}{2}+\frac{\pi^2T^2}{\theta_D^2}\right)\right]$$

$$\text{for} T \geq \frac{\theta_D}{2}$$

$$f = \exp\left[\frac{-6E_RT}{K_B\theta_D}\right]$$

The above equation indicates that the probability for Mössbauer effect increases with

(I) Decrease in recoil energy

(II) Decrease in temperature

(III) Increase in Debye temperature θ_D

2.4 Mössbauer Parameters :

In a Mössbauer experiment the source and the absorber are moved relative to each other in a controlled manner and transmitted γ-rays are registered as a function of relative Doppler velocity. Resonance occurs only at some particular relative velocity. From the observed spectrum a number of parameters can be obtained. They are

1) Electromagnetic Parameters :

These parameters depend on the Hyperfine interactions of the nucleus and the extranuclear fields. The coulomb interactions of the nuclear charge with the s-electrons result in Isomer shift of resonance line.

Also one can have quadrupole interactions for quadrupole moment of the nucleus and the Electric field gradient in the solids resulting in splitting of the lines. Magnetic interactions can also take place due to interaction of magnetic dipole moment of the nucleus and the extranuclear magnetic fields resulting in zeeman splitting of spectral lines.

2) Dynamic Parameters.:

These parameters depend on the dynamics of the motion of the emitting and the absorbing nuclei in the solids. The f-fraction, line broadening, second order Doppler shift are some of the examples.

3) Combined Parameters :

It is possible that both the electromagnetic interactions detailed above and also the dynamics of the motion of the nuclei may be present in the same system.

2.5 Isomer Shift (IS):

Electric monopole interaction takes place between the nuclear charge, which has a finite volume and the electrons nearest to the nuclear region. The electrostatic coulomb interaction takes place due to the probability of S electrons penetrating the nucleus and spending a fraction of their time there. The electric monopole interaction changes the energy of the atoms by an amount

$$\delta E = W\varphi - W_0$$

Where $W\varphi$ is the electron interaction energy due to finite nuclear size and W_0 is due to point nucleus. The energy due to coulomb interaction is

$$E_I = \frac{2}{3}\pi Z e^2 |\psi(0)|^2 \langle r^2 \rangle \equiv \delta E$$

Where δE is to express very small change in energy.

For each nuclear state the nuclear volume and hence the quantity $\langle r^2 \rangle$ is different. Hence for a nuclear transition between a ground state and excited state the energy change of a γ-ray will be

$$\Delta E = E_s - E_0 = (\delta E)_e - (\delta E)_g$$

$$= \frac{2}{3}\pi Z e^2 |\psi(0)|^2 \left[\langle r^2 \rangle_e - \langle r^2 \rangle_g \right]$$

where suffixes s means source, e the excited state and g the ground state.

In Mössbauer effect, $(\Delta E)_A$ and $(\Delta E)_S$ are not observed separately but only the difference of the energy shift in the source and absorber is observed. The electron density at the nucleus is influenced by any change in temperature, structure, pressure, electronic configuration etc. Hence

$$= \frac{2}{3}\pi Ze^2\left[|\psi(0)|_A^2 - |\psi(0)|_S^2\right] \quad \left[\langle r^2\rangle_e - \langle r^2\rangle_g\right]$$

$$\delta = (\Delta E)_A - (\Delta E)_S$$

Where δ known as Isomer Shift.

If atomic nuclei are considered spherically symmetric having radius R and charge density $\rho_n(r)$

$$\delta = 4\pi Ze^2\left[\,|\psi(0)|_A^2 - |\psi(0)|_S^2\right]\left(\frac{\delta R}{R}\right)R^2$$

Then $\rho_n(r) = 3Ze/4\pi R^3$

Where $\delta R = R_e - R_g$ and $2R = R_e + R_g$

The corresponding Doppler velocity V_D that is necessary to restore resonance between the source and the abosrber in a Mossbauer experiment is given by

$$V_D = \left[\frac{4\pi C}{5E\gamma}\right] Ze^2R^2\left(\frac{\delta R}{R}\right)\left\{\left|\psi(0)\right|_A^2 - \left|\psi(0)\right|_S^2\right\}$$

V_D can be calculated from Mossbauer spectra as distance of resonance line or centroid of resonance multiplet from zero Doppler velocity. The details of the theory can be found in ref. (2-4)

The nuclear factor δR/R depicts relative change of the nuclear radius going from excited to ground state.

The positive value of the Isomer Shift indicates electron density at the nucleus increases in going from source to absorber, and negative value indicates that electron density at the absorber nuclei is lower than at the source nuclei. For constant nuclear part one can directly infer about the electronic environment of the nucleus. The value of IS depends on changes in s-electron density. Hence it provides information regarding the chemical surroundings of the Mossbauer isotopes. Changes in oxidation state, spin states etc. can influence the electronic structure, which will have direct bearing on the value of Isomer shift (5).

2.6 Second Order Doppler Shift:

The Isomer shift has a temperature dependence was pointed out independently by Pound and Rebka (6) and Josephson (7). The relativistic equation for Doppler effect on an emitting photon gives the observed frequency

$$\nu' = \nu(1-V/C)\,(1-V^2/C^2)^{-1/2}$$

This equation can be approximated as

$$\nu' = \nu(1-V/C)\,(1+V^2/2C^2)$$

Where ν is the frequency of the stationary system.

For first order, Doppler effect is zero as mean velocity of vibration averages to zero.

The second order term $\nu' = \nu\,(1+V^2/2C^2)$ will contribute to the shift in resonance line by $\delta E_\gamma/E = -\langle V^2\rangle/2C^2$

This contribution given by the equation is referred to as second order Doppler shift (SOD). The Isomer shift measured in Mössbauer experiments contains two terms, one which does not contain the second order Doppler shift δ_C and the other that contains second order Doppler Shift.

i.e. $\delta = \delta_c + \delta_{SOD}$.

The second order Doppler Shift can be estimated if the effective Debye temperatures of the Source and absorber are known. SOD Shift values for a number of different isotopes are given in references. (8)

2.7 Quadrupole Splitting :

When the electric quadrupole moment Q interacts with the principal component of the diagonalized electric field gradient (EFG) tensor Vzz = $\partial^2 V/\partial z^2$ at the nuclear site, a split in the nuclear level takes place with the eigen values

$$E_Q = \frac{eQV_{ZZ}}{4I(2I-1)}\left[3m_I^2 - I(I+1)\right]\left[1+\frac{\eta^2}{3}\right]$$

The asymmetry parameter η =(Vxx - Vyy)/Vzz

With |Vzz| ≥ |Vyy| ≥|Vxx| ; and $V_{xx} + V_{yy} + V_{zz} = 0$

The electric quadrupole interaction splits the nuclear excited state of Fe^{57} (I=3/2) into sublevels, as shown in the energy level diagram (2.1A) having the eigen value

$$E_Q = \pm\frac{1}{4}eQV_{ZZ}\left(1+\frac{\eta^2}{3}\right)^{\frac{1}{2}}$$

Hence as a result of the splitting of the 3/2 level, the emission spectrum will consist of two components corresponding to the ±3/2 to ±1/2 and ±1/2 to ±1/2 transition. Here two lines may be observed in the velocity spectrum.

A totally resolved quadrupole doublet in the spectrum will be observed in case when $|E_Q(\pm 3/2 \rightarrow \pm 1/2)| + |E_Q(\pm 1/2 \rightarrow \pm 1/2)| >> 2\Gamma$ where Γ is the line width. The energy difference between the lines of the doublet is $\Delta EQ = \pm eQV_{ZZ}/2$. The product eQV_{ZZ} is called the quadrupole coupling constant. The product $|QV_{ZZ}|$ can be obtained from the observed splitting of the experimental data. By measuring the ratio of the intensities of $(\pm 3/2 \rightarrow \pm 1/2)$ and $(\pm 1/2 \rightarrow \pm 1/2)$ transitions as a function of angle observed relative to the Z-axis in case of a single crystal and using the relation

$$\frac{M_{\pm\frac{3}{2}\rightarrow\pm\frac{1}{2}}}{M_{\pm\frac{1}{2}\rightarrow\pm\frac{1}{2}}} = 3\left[\frac{1+\cos^2\theta}{5-3\cos^2\theta}\right]$$

it is possible to identify the lines.

2.8 Magnetic Splitting:

If an external magnetic field is acting at the site of a nucleus having a non-zero magnetic moment, the energy of the state will change, because of the magnetic interaction, by a value given by

$$E_M = -\mu.H = -g\,\mu_N\,H\,m_I$$

Where μ_N is the nuclear magneton, g is the nuclear g-factor and m_I is the magnetic quantum number representing the Z-component of the nuclear spin. The magnetic field splits the nuclear level into (2I + 1) equispaced sublevels. The transition can take place between different nuclear sublevels if $\Delta m_I = 0, \pm 1$. The allowed transition for 3/2 → 1/2 gamma ray are shown in figure (2.1B)

In a Mössbauer experiment with a single line source and a magnetically ordered substance as an absorber, one can observe a resonance sextet, centroid of which may be shifted from the zero velocity. The effective hyperfine magnetic field at the probe nucleus can be found by magnetic hyperfine splitting. There are a number of factors that contribute to the effective magnetic field. If in some cases both magnetic field as well as static electric field gradient are present simultaneously at the nucleus, the position of the sublevels of the hyperfine structure will depend on the ratio of the magnetic to the electric interaction, direction of the magnetic field, symmetry of the electric field gradient and the angle between the principal axis of the field gradient and the magnetic axis.

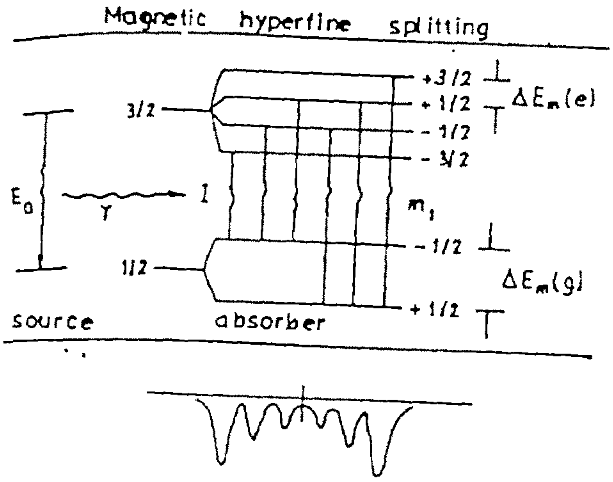

Fig. 2.1 B Interaction of the nuclear dipole moment with a magnetic field at the nucleus

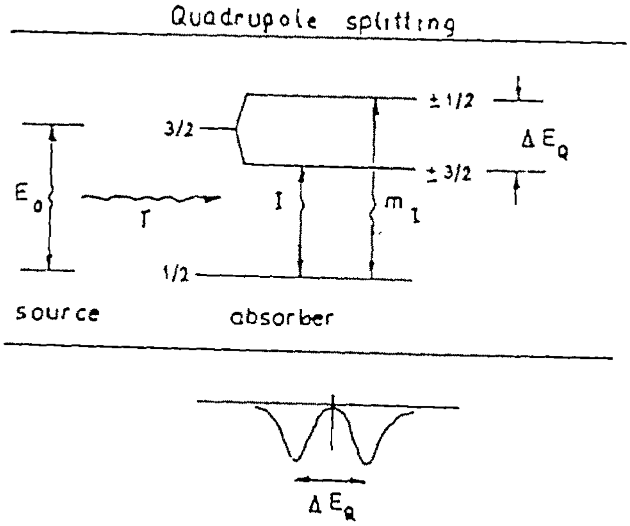

Fig. 2.1 A Interaction of nuclear quadrupole moment with EFG at the nucleus

In case of combined electric and magnetic interactions, the interpretation of the Mössbauer spectrum can be quite complex. Details of these types of interactions can be found. (9)

2.9 Line Shape and Resonance Intensity:

The resonance Intensity observed in the Mössbauer spectrum depends on the resonance cross section (10) and the effective thickness of the absorber.

$$t = n f_{abs} \sigma_0$$

where n is the number of atoms of the Mössbauer nuclei per square centimeter, f_{abs} is the recoil free fraction. If the nuclear levels are split due to hyperfine interactions, the resonance cross section σ_0 is divided among the different transitions and effective value of t decreases accordingly.

The line shape of a Mössbauer spectrum is of Lorentzian type. In Mössbauer experiment, the source as well as the absorber has each a line width Γ associated with them and hence the minimum width observed should be 2Γ. But actually the line width observed in experiments are usually more than 2Γ. This is due to inhomogeneous broadening or the thickness broadening. The inhomogeneous broadening occurs due to imperfections in the source and absorber. The thickness broadening arises due to the fact that for thick absorber the absorption effect at the centre of the resonance saturates before, than in the wings thus making the observed spectral line wider. The thickness effects are discussed in detail by Schwartz (11) and by Dhenoy (12). The widening of the resonance line can also take place due to two or more inequivalent sites for the probe nucleus.

2.10 Parabolic Effect:

One more effect known as the parabolic effect also widens the line width. A moving source causes periodic changes of the source-detector Solid angle and the count rate will be a parabolic function of the source velocity. The magnitude of this geometric effect strongly decreases with the ratio of the source vibration amplitude to the source detector separation. In constant acceleration mode with a triangular wave drive, the magnitude of the parabolic effect have opposite signs in the two halves and this effect can be minimized by folding the two Mössbauer spectra, which are mirror images of each other.

2.11 Magnetic Properties :

Studies to understand the Magnetic Properties in solids have led to the fundamental structures of these materials. A variety of experimantal techniques like the Bulk Magnetization, susceptibility measurements, Mössbauer, ESR, NMR techniques, neutron diffraction etc. have led to this progress of understanding the basic properties in them. Detailed Magnetic properties can be found out by using any one or a combination of more than one of the above techniques, like the combination of microscopic measurement by the Mössbauer Effect and also neutron diffraction to get an elaborate picture.

The ferromagnetism seen in 3d-transition metals like Fe, Co, Ni, etc and that in rare earths is quite different. The difference lies in the filling of the orbitals. In the case of 3d-transition metals the electrons in the partially filled 3d shells give rise to the magnetism whereas in case of rare earths it is due to the partially filled 4f states which are responsible for the magnetic properties. The 4f shells are deep inside but the 3d electrons are more exposed to the surrounding environment and hence can take part in bond formation. Thus the magnetism in these system should take into the wandering nature of these electrons in the case of the transition metals and alloys.

The ferromagnetism is the case of highly ordered state. But the case of anti ferromagnetism is that of highly aligned one. Here the atomic moments are aligned as in the case of ferromagnet, but the individual moments are arranged in a self-compensatory way so that the overall spontaneous magnetism is nullified. Considering the crystal as divided into two sub-lattices arrives at this situation. The arrangement of spins is such that if the spin of one of the sub lattices is in a particular direction, the spin of the other is exactly in the opposite direction. The spins of the nearby moments are always antiparallel such that the over all spontaneous magnetization is zero. In materials, which exhibits Ferrimagnetism, the arrangement of the spins of the sublattices are largely in opposite direction but not perfectly of equal magnitude. Hence there is a net spontaneous magnetization. The behaviour of the magnetization with temperature allows the classification of ferromagnetic and of anti ferromagnetic material.

2.12 Theories of Ferromagnetism :

Ewing (13) was amongst the first few who tried to explain the phenomenon of ferromagnetism in terms of the forces between atoms. He assumed that each atom was a permanent magnet free to turn about its centre in any direction. The orientations of various magnets in the field and also with respect to each other were supposed to be entirely due to mutual magnetic forces. Using this model he could explain phenomena like the magnetisation curves and hysteresis loops associated with it.

But a serious discrepancy was found when the thermal energy was compared with the magnetic potential energy estimated by this model. It was estimated that the thermal energy was two hundred times more than that of the calculated magnetic field. (14) . This implies that even at very low temperature the thermal energy will not allow the atomic magnets to form any stable configuration. Hence from this it can be said that there must be some additional force which makes the material ferromagnetic.

The Weiss (15) theory of ferromagnetism introduces a molecular field to account for the nature of the atomic forces which gives rise to ferromagnetism. He made the assumption that :

1. The elementary magnets are subjected to thermal agitation and may have any orientation with respect to the field.
2. These magnets are very far from each other. Hence there is no influence of one over other.

Suppose that these elementary magnets have each a magnetic moment μ_A and are in the field of strength H.

The energy due to the field can be written as

$$W = -\mu_A H \cos\theta$$

for each dipole oriented so that μ_A makes an angle θ with the field H. When the ensemble is subjected to thermal agitation at a certain temperature T, the number of dipoles oriented in the solid angle $d\omega$ about the direction θ is proportional to

$$e^{-W/kT}\, d\omega = e^{(\mu_A H\cos\theta)/kT}\, d\omega$$

Using the equation of W we get

$$\frac{\overline{\mu_A}}{\mu_A} = \coth\left[\frac{\mu_A H}{KT}\right] - \frac{KT}{\mu_A H}$$

$$or \frac{I}{I_0} = \tanh\left[\frac{I/I_0}{T/\vartheta}\right]$$

Where μ_A is the average dipole moment, k the boltzman's constant and I_0 is the intensity of magnetisation at 0^0 K. The introduction of Quantum theory made some alterations to the first assumption. It only allowed certain discrete orientations of moments instead of moments having random distribution. If there are J values of the total spins of the ensembles, then the number of magnetic moments with respect to the magnetic field is 2J+ 1. Then the expression I/I_0 is modified.

It was shown by Heisenberg (16) that the molecular field postulated by Weiss can be explained in terms of Quantum mechanical forces of exchange acting between electrons in neighbouring atoms. As two atoms are brought near to each other from a distance, these forces cause the electron spins in the two atoms to become parallel (ferromagnetism). As the atoms are brought nearer together the spin-moments are held parallel more firmly until at a certain distance the force diminishes and then becomes zero. Still closer the spins set themselves antiparallel (antiferromagnetism).

2.13 Magnetic Hyperfine Interactions :

The interaction between the magnetic field intensity B and the nuclear magnetic moment μ is described by the Hamiltonian

$H = -\mu . B$

The magnetic moment μ is parallel to the nuclear spin I which allows the introduction of nuclear g-factor

$\mu = g\mu_N I$

where $\mu_n = 0.50508 \times 10^{-27}$ JT^{-1}, is the nuclear magneton. The magnetic field B can be written as B_{HF}, the hyperfine field. In the presence of external field B_{ext} the expression for B becomes modified to include the external field and the demagnetising field ($-\mu_0 DM$). Hence

$$B = B_{HF} + B_{ext} - \mu_0 DM.$$

Here the hyperfine field includes the Lorenz field $1/3\mu_0 M_s$, M_s the saturation magnetization and M is the magnetisation of the sample. If the positive Z –axis is chosen along the direction of the field B, then the eigen value can be written as $E_m = m\hbar\omega_L$ where ω_L is the larmor precision and $\omega_L = -g\mu_N B/\hbar$.

In classical description this is the precession frequency of the nuclear spin around the magnetic field. The negative sign indicates the precession to be according to the right hand rule.

External magnetic field of the order of 10T cannot be produced easily but the hyperfine field of diamagnetic impurities in ferromagnetic materials can reach values of 100T. Hence one can see that impurities in a crystal are subjected to fields higher than what can be applied externally.

The hyperfine field is predominantly caused by the net spin density at the nucleus and the magnetic field can be written as the sum of three contributions namely conduction electron polarization (cep) , core polarization (cp) and overlap polarization (op).

i.e. $B_{HF} = B_{cep} + B_{cp} + B_{op}$

The theories showing these effects are semi-empirical in nature. (17,18,19).

The core polarization occurs when a partly filled atomic d-shell is polarized by the conduction electrons of the host, which in turn polarizes the inner s-electron of the impurity atom. As the contact density of the s- electron is large, the resulting magnetic hyperfine field may be quite strong.

The conduction electron polarization contribution to the hyperfine field on Fe in Fe host is found to be due to RKKY-oscillations (20, 21). Its value is of the range –14 T to –22 T (22). For non magnetic impurity the value of the conduction electron polarization is approximately the same as that of Fe, provided the impurity is of the same row and the effective impurity charges ΔZ is close to zero.

A model developed by Stearns (21) assumes the cep contribution to vary little with ΔZ and the positive shift in B_{HF} with increase in ΔZ was attributed to volume misfit effect. She said that influence of a charge perturbation is small and can not contribute to cep. Where the influence of the non magnetic neighbours on the magnetic host Fe is considered this holds true. Examples are the Fe-Al and Fe-Si systems.

Dewaard et. al. (23) found large hyperfine field shift for sp-impurities in Fe, Co and Ni hosts where these impurity atoms trap a number of vacancies. The extra phase term in cep formula given by Campbell and Blandin (19) was justified by Daniel and Friedel (24). They assumed a positive average polarization of the conduction electrons. The excess impurity charge ΔZ is screened by conduction electrons. Conduction electrons scattered by the impurity potential set up the screening charge, which is deeper for the spin down than the spin up electrons. The screening charge density shows up an oscillatory behaviour determined by the product of the conduction electron spin density and the scattering potential for spin up and spins down respectively.

2.14 Local moments and Dilute Alloys:

The transition metals and rare earths show a variety of magnetic phenomena when they are incorporated in some systems. The magnetic susceptibility generally shows a Curie-Weiss behaviour. The magnetic properties in these systems are due to the individual transition metals or rare earth ions. Hence the study of localized and stable magnetic moments on the transition metals forms an important area of magnetism. The magnetic moment on the d ion in a host can survive if coulomb interaction energy is greater than the virtual line width arising from the hybridization with the conduction electrons i.e. intra atomic correlation favours magnetic moment. The d electrons in 4d transition metals generally don't show tendency towards moment formation. When a transition or a rare earth metal atom is present as an impurity in a system, the electrons in its outer s and p shells form a part of the conduction band and the impurity is left with partially filled d or f levels. But the impurity in a metallic host can make hybridization with its d or f electrons. In this case the Hund's rule ceases to be the ground state and the magnetic moment may or may not survive. If the moment survives then it may or may not be stable. For example Fe is non magnetic in Al, but shows a magnetic moment of ~1μ_B with spin fluctuation temperature θ~30K in Ti. Similarly Fe shows a stable moment of 3μ_B in Au at θ~0K.

Hence a moment can survive at what conditions has to be answered. J. Friedel (25) had done theoretical calculations on magnetic impurities in metallic host. His work indicated that of a virtual bound state i.e. a state that is almost localized due to resonant scattering at the impurity site. In this state the electrons spend a relatively larger portion of the time in this region around the impurity but are not in a bound state. Virtual bound state resonance occurs for the transition metal or rare earth impurities when the d or f levels lie with in the conduction band of the metal host.

A different approach was given by P.W. Anderson (26). He started with the atomic d or f wave functions of the impurity ion and then modified it in the presence of the neighbouring metal ions of the host metal. The Anderson model contains in addition to a narrow resonance associated with impurity states, a short range repulsive interaction between the impurity electrons. This interaction is essential to explain the observation of the localized moments. If the local moment on the impurity exists, the Anderson model can be transformed into Kondo model (25). This model indicates antiferromagnetic interaction between the spin of the conduction electrons and the spin of the impurity. In a static scenario, the antiferromagnetic interaction gives rise to a screening of the local spin by the surrounding cloud of conduction electrons with opposite sign which can lead to the disappearance of magnetism at low temperatures.

It is not an easy task to determine experimentally the behaviour associated with a single impurity. Bulk measurements like magnetic susceptibility, specific heat, resistivity provides information on macroscopic scale. In order to get information about the impurity behaviour, the contribution to the above measurements arising from the host has to be estimated. Also inter impurity interaction poses a problem while extracting single impurity behaviour, especially in case of transition metals impurities. The strong exchange interaction between the transition metal impurities due to direct overlap of the outer d shells can result in magnetic ordering and 'frozen magnetic moment', which can not take part in Kondo scattering.

Extensive studies were carried out for the 3d impurities in several hosts by PAD method. These studies revealed that the characteristic features of magnetic moments are strongly influenced by the type of conduction electrons of the hosts (27). IF Fe develops a magnetic moment in a host metal having s or sp conduction band, it always shows positive local susceptibility (28). The positive value of hyperfine field arises due to the large contribution from the orbital moment of Fe. The magnetic behaviour of Fe in these types of hosts can be called 'ionic type' behaviour. Here the crystal field is of less importance.

The spin fluctuation temperature T_{sf} increases rapidly with decrease in the cell volume of the host. Thus, as the hybridization between the Fe 3d and the host increases, the spin fluctuation temperature also increases.

In noble and d band metal hosts, Fe shows negative local susceptibility which is due to negative hyperfine fields through core polarization. The correlation between the host volume and the spin fluctuation temperature seen in case of sp host is absent in case of Fe in noble and d band hosts. By this trend one expects a very high value of spin fluctuation temperature for Fe in Au due to small cell volume of Au. But a stable moment with spin fluctuation temperature of ~0 ^{o}K has been observed in case of Fe in Au. This was explained on the basis of ferromagnetic exchange interaction between the Fe and the neighbouring Au ions, which suppresses the spin fluctuation arising from the antiferromagnetic exchange interaction between the Fe 3d and the host conduction electrons (29).

2.15 A brief theory of superconductivity

2.15 A Introduction:

Superconductivity is a remarkable phenomenon that occurs in many metals and alloys at low temperature. Below a certain temperature called the critical temperature T_C the resistance to the flow of electricity through the conductor vanishes completely. This phenomenon was originally discovered by K. Onnes in 1911 in metallic mercury at 4.2 K. Since then a large number of metals, alloys, compounds have been found to show the property of superconductivity. In addition to zero electrical resistance, superconductor exhibits Miessner effect where by a superconductor expels magnetic flux from within and becomes a perfect diamagnet till a critical applied external field. Till 1986 though many compounds were developed but the T_C was only around 24 K. In 1987 copper based mixed oxide systems were discovered which for the first time raised the T_C of the superconductors to above liquid nitrogen (>77K) temperature.

Superconductors can be classified into type I and type II depending on their response to an external magnetic field. As mentioned a superconductor expels the magnetic flux from within.

That is

$$B = H + 4\pi M; \qquad \chi = M/H = -1/4\pi$$

Where B is the magnetic induction or flux density, M is the magnetization or magnetic moment per unit volume, H is the magnetic field and χ is the magnetic susceptibility. Thus, in the superconducting state, χ is negative and a plot of $-4\pi M$ Vs H is a straight line (fig 2.1C). However when $H = H_C$, the critical magnetic field, the superconductivity is destroyed, even though $T < T_C$ and flux will penetrate. Many superconductors exhibit this property and are called type I superconductors. Here the value of H_C varies from 10-500Oe depending on the material.

But many superconductors including the ceramic superconductors, exhibits the type II behaviour. In this case superconductor passes from a perfect diamagnetic state at low magnetic fields to a mixed state and finally to a 'sheathed' state before attaining the normal state of the metal (fig 2.1D). The magnetic field values correspond to H_{C1}, H_{C2} and H_{C3}. The superconducting state below H_{C1} is perfectly diamagnetic and identical to a type I behaviour. In the region between H_{C1} and H_{C2}, the material is in a mixed state in which the superconducting region is enclosed by normal region. H_{C2} values are of the order of 10-200Koe. Ceramic superconductors like $YBa_2Cu_3O_7$ has H_{C2} values of the order of 1500-2000K Oe.

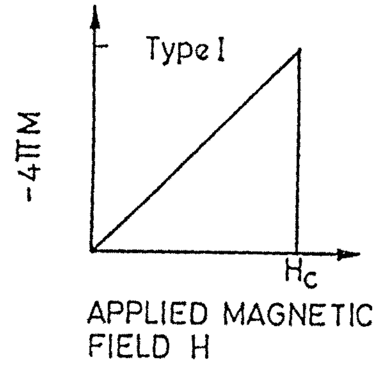

Fig. 2.1 C

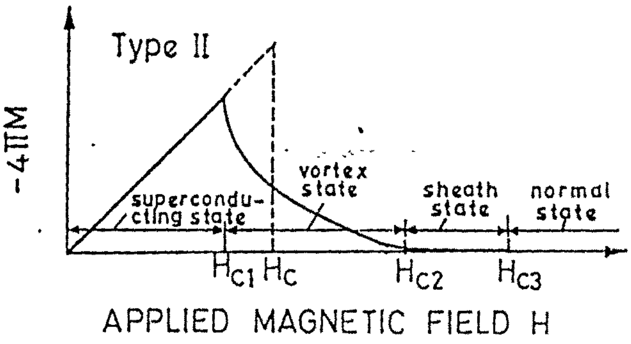

Fig. 2.1 D

Magnetization curves for (a) Type I and (b) Type II superconductor.

The Ginzburg-Landau-Abrikosov-Gorkov (GLAG) theory satisfactorily explains the behaviour of type II superconductors by using the concept of penetration depth and coherence length. The penetration depth (λ) is defined as the distance upto which the magnetic flux can penetrate in an applied magnetic field and is usually 500-1500 A. In the superconducting state under an applied magnetic field there is a distance over which a coherence of superconducting state exists and this range of coherence is known as coherence length ξ, usually of the order of 1000-3000A. According to GLAG theory, the dimensionless quantity GL parameter (κ) is defined as $\kappa = \lambda/\xi$,. For a type I superconductor $\kappa < \frac{1}{\sqrt{2}}$ where as for a type II superconductor $\kappa > \frac{1}{\sqrt{2}}$. Thus for a type II superconductor, the magnetic field penetrates farther than the coherence length into the superconductor.

2.15B BCS Theory:

Superconductivity is a quantum phenomenon where electronic motions are correlated over macroscopic distances. The most successful theory is microscopic one proposed by Bardeen, Cooper and Schriffer (BCS) in 1987. According to BCS theory, an electron in a metal interacts with another electron via the phonons (lattice vibrations). When this attractive interaction exceeds the natural coulomb repulsion between the two negatively charged electrons, there will be a weak binding between them resulting in the formation of spin and also momentum paired electrons (cooper pairs). This cooper pair formation opens up an energy gap (2Δ)at the fermi level in the metal when cooled below T_C. (fig 2.1E), the value of which depends on different types of superconductor. Many properties like zero resistance, Messiner effect, Isotope effect ($T_C \propto [M]^{-0.5}$ where M is the isotopic mass) etc. can be accounted for by the existence of cooper pairs.

According to the BCS theory, the T_C is given by :

$$T_C = 1.14\,\theta_D \exp\left(\frac{1}{N(0)V}\right)$$

Where θ_D is the Debye temperature, which is related to the average resonance frequency of the lattice (ω_D) by $\hbar\,\omega_D = K\,\theta_D$... $N(0)$ is the density of the states at the fermi level per spin and V is the net pairing potential arising from the electron phonon interaction. The BCS equation holds for weakly coupled superconductors and doesn't hold in strict sense for materials where electron-phonon coupling is strong (i.e. $T_C / \theta_D = 0.1$)

Eliashberg, McMillan, Allen and Dynes extended the BCS theory taking into account the coulomb repulsion between the electrons. Though the BCS theory and its extensions can explain the Tc and related properties, it has a few limitations.

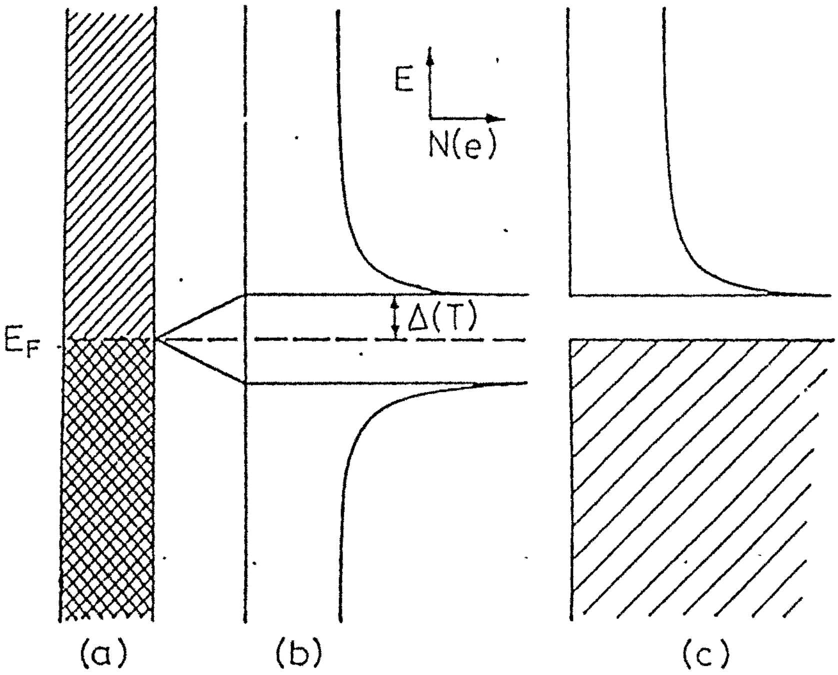

Fig. 2.1 E

Density of states at the Fermi level (E_F):

(a) Normal state (b) Superconducting state.

(c) ground state pairs in superconducting state explicitly shown.

The isotopic effect is apparently absent or considerably reduced in some transition metal superconductors and their alloys. Also the effect of pressure on the T_C of transition metal superconductors doesn't correlate well with the θ_D as it does in non transition metal superconductors.

The BCS mechanism assumes phonons as the mediators for the formation of Cooper pairs. Several other (non BCS) mechanism have been proposed which leads to electron-electron attraction and formation of Copper pair. The notable ones are the excitonic (electron excitation), acoustic plasmons and spin excitons.(30-36).

References:

1. .L. Mossbauer, Z. Physik, vol. 151, 1958, p-124.
2. Greenwood, N.N., and T.C. Gibb ; Mossbauer Spectroscopy, (Chapman and Hall Ltd., London, 1971).
3. Werthiem, G.K., Mossbauer Effect : Principals and Applications, Academic Press, New York, 1964.
4. Benozer-Koller, N and R.H. Herber, "Chemical Application of Mossbauer Spectroscopy" eds. V.I. Goldanskii and R.H. Herber, Academic press, New York, 1968.
5. Shenoy, G.K. and F.E. Wagner, "Mossbauer Isomer Shifts" , North Holland, Amsterdam, 1975.
6. Pound, R.V. and G.A. Rebka, Phys. Rev. Lett., 4 (1960), p-274.
7. Josephsen, B.D., Phys. Rev. Lett., 4 (1960), p-341.
8. Gettys, W.L. and J.G. Stevens, In C.R. C. Handbook of Spectroscopy, Vol. III,
9. Ed. By J.W. Robinson, CRC Press, Florida, 1981.
10. Goldanskii, V.I., and E.F. Makarov, "Chemical Applications of Mossbauer Spectroscopy"; ed. By I. Goldanskii and R.H. Herber, Academic Press, New York, 1968.
11. Alder K., Phys. Rev. 84 (1951), p-369.
12. Schwartz, L.H., "In Application of Mossbauer Spectroscopy", ed. By R.L. Cohen, Academic Press, Vol. I, p-37.

13. Shenoy, G.K., J.M. Friedt, H. Maletta and S.L. Ruby; In " Mossbauer effect Methodology"; ed. By I.J. Gruverman, Plenum, New York, 1975, Vol. 9, pp. 277.

14. Ewing, J.A, Phil. Mag. Vol. 43, 1922, p-493.

15. Crangle, J., "The Magnetic Properties of Solids", Edward Arnold Ltd., London, 1977.

16. Weiss, P., Ann. de. Phys., Vol. I, 1914, p- 134.

17. Heisenberg, W., Z. Physik, Vol. 49, 1928, p-619.

18. Jena, P. and J.M. Geldart, J. Mag. and Mag. Mat., Vol. 8, 1978, p- 99.

19. Stearns, M.B. and J.M. Norbeck ; Phys. Rev., Vol. B20, 1979, p-3739.

20. Campbell, I.A. and A. Blandin; J. Mag. and Mag. Mat., Vol. I, 175, p –1.

21. Watson, R.E "In Hyperfine Interactions" , Eds. A.J. Freeman and R.B. Frankel, Academic Press, New York, Chapter 9, 1967.

22. Stearns, M.B, Phys. Rev., Vol. B11, 1971, p-4081.

23. Arends, A.R, Ph.D. Thesis, University of Groningen, Netherlands, 1981.

24. De Waard, H. and F. Pleiter, L. Nelsen and D. Hafemester, Hyp. Int., Vol. 9, 1981.

25. Daniel, E. and J. Friedel, J. Phys. Chem. Solids, Vol. 24, 1963, p-1601.

26. J. Friedel, Nuovo Cim.(Suppliment), 7,287, 1958.

26 P.W. Anderson, Phys. Rev., 124, 41, 1964.

27. D. Riegel and K.D. Gross, Physicca B, 163, 678, 1990

28. D. Riegel, L. Buermann, K.D. Gross, M. Luszik-bhadra and S.N. Mishra, Phys. Rev. Lett., 61, 2129, 1988.

29. D. Riegel, L. Buermann, K.D. Gross, M. Luszik-bhadra and S.N. Mishra, Phys. Rev. Lett., 62, 316, 1989.

30. R.D. Parks (Ed.) 'Superconductivity' Vol. I and II, Marcel Dekker, NY, 1969.

31. C. Kittel, 'Introduction to Solid State Phys.', John Wiley, NY, 1971.

32. M. Tinkham, 'Introduction to Superconductivity' Mcgraw Hill, NY, 1975.

33. C.N. Rao and K. J. Rao, 'Phase transitions in Solids', Mcgraw Hill, NY, 1978.

34. A.V. Narlikar and S.N. Ekbote, Superconductivity and Supercond. Materials', South Asian Publ., New Delhi.

35. C.N.R Rao and J. Gopalakrishnan, 'New Directions in Solid State Chemistry', Cambridge Univ. press, Cambridge, 1986.

36. N.P. Ong : 'Physical properties of High T_C superconductors' II edition, Ed. D.M. Ginzburg, World Scientific, Singapore.